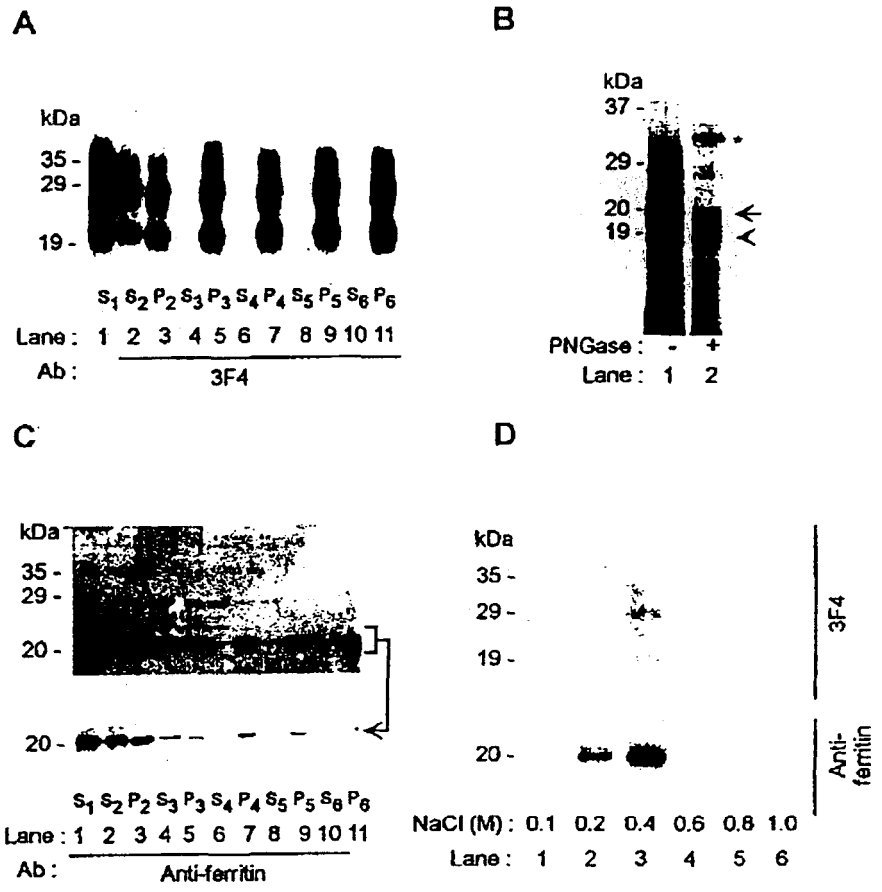

Figure 4. Protease-resistant sCJD–PrP^{Sc} is associated with ferritin. Clarified supernatant obtained from PK-treated CJDH (S1) was subjected to five additional rounds of ultracentrifugation, and the resulting detergent-soluble supernatant (S2–S6) and detergent-insoluble pellet (P2–P6) fractions were immunoblotted with 3F4. *A*, The starting material (S1) and the supernatant and pellet fractions obtained after ultracentrifugation (S2 and P2, respectively) show the N-terminally truncated PrP^{Sc} glycoforms migrating at 29 and 30, 22–25, and 19 kDa, respectively (lanes 1–3). After the first round of ultracentrifugation, 60% of PrP^{Sc} fractionates in the pellet fraction (lanes 2, 3). After subsequent rounds of ultracentrifugation, all of the PrP^{Sc} is detected in the pellet fractions (lanes 4–11). *B*, Silver staining of the P6 fraction shows PrP^{Sc} glycoforms of 19–30 kDa and a 20 kDa band (lane 1). After treatment with PNGase, all PrP^{Sc} glycoforms migrate at 19 kDa, as expected (lane 2, arrowhead), whereas the 20 kDa band remains insensitive to deglycosylation (lane 2, arrow). The slower migrating band in lane 2 (*) is derived from the added PNGase. *C*, Reprobing of the membrane in *A* with anti-ferritin antibody shows strong immunoreaction with the 20 kDa band and minor species migrating at 25 and 30 kDa (lanes 1–11). The 20 kDa band is detected in the first three fractions (lanes 1–3) and in all subsequent pellet fractions (lanes 4–11). *D*, The P6 fraction from *A* was treated with NaCl and subjected to DEAE-cellulose chromatography. Immunoblotting of eluted proteins with 3F4 and anti-ferritin antibodies shows dissociation of ferritin from PrP^{Sc} at concentrations of 0.2–0.4 M NaCl (lanes 2, 3).

amounts of 3F4-immunoreactive PrP^{Sc} from CJDH-DE and a small amount from CJDH sample coimmunoprecipitates with anti-ferritin (Fig. 5*A*, lanes 3, 4). Reprobing of the same membrane with anti-ferritin reveals the H and L chains of ferritin migrating at 21 and 20 kDa, respectively (Fig. 5*A*, lanes 5–8). In the CJDH-DE sample, additional slower migrating bands that react strongly with anti-ferritin antibody are detected (Fig. 5*A*, lane 8). Their identity is not clear at present. Immunoprecipitation of CJDH-DE with 8H4, followed by probing with 3F4 or anti-ferritin antibodies, shows similar association of PrP^{Sc} with ferritin (Fig. 5*A*, lanes 9, 10). The apparent difference in the amount of PrP^{Sc} and ferritin that coimmunoprecipitate with anti-ferritin versus 8H4 is probably attributable to the nature of the specific antibodies (N. Morel et al., 2004). DE treatment partially hydrolyzes the H chain of ferritin, which comigrates with the L chain at 20 kDa (Fig. 5*A*, lane 5 vs 6, 7 vs 8).

Silver staining of anti-ferritin- and 8H4-immunoprecipitated proteins from DE-treated NH and CJDH shows bands comigrating with ferritin at 20 kDa and several unidentified proteins (Fig. 5*A*, lanes 11–14). No PrP was immunoprecipitated in the absence of primary antibody from either mock-treated or DE-treated NH or CJDH, confirming that PrP^{Sc} does not bind nonspecifically to protein A beads (Fig. 5*B*).

sCJD–PrP^{Sc} is cotransported with ferritin across Caco-2 cells

To determine whether PrP^{Sc} is transported across Caco-2 cells in association with ferritin, 20 μl of CJDH-DE in serum-free medium was added to the AP chamber of filter inserts containing Caco-2 cell monolayers and incubated for 2 hr at 37°C. At the end of the incubation, monolayers were cut into two pieces: one half was immunostained for PrP and ferritin, and the other half was immunostained for the tight junction protein ZO-1. Transport of PrP and ferritin was checked by capturing horizontal confocal images at different depths as depicted in Figure 6*A* and by taking vertical images.

Staining for PrP (green) and ferritin (red) at level I shows colocalization of PrP and ferritin (Fig. 6*B*, panels 1–3, arrows) and limited reactivity for PrP alone (Fig. 6*B*, panels 1, 3, arrowheads). Similar images captured at level II (at the level of the filter pores) also show colocalization of PrP (green) and ferritin (red) (Fig. 6*B*, panels 4–6, arrows). Immunostaining for the tight junction protein ZO-1 (green) reveals intact tight junctions throughout the Caco-2 monolayer (Fig. 6*B*, panel 7). A vertical image through the same cells shows colocalization of PrP (green) and ferritin (red) at the AP and BL membranes (levels I and II) (Fig. 6*B*, panels 8–10). Transport of both PrP^{Sc} and ferritin was significantly inhibited by incubation at 18°C and by pretreatment of the cells for 2 hr with brefeldin-A (3.5 μM) or nocodazole (33 μM), implicating a transcytotic process (data not shown).

sCJD–PrP^{Sc} remains associated with ferritin after transcytosis

To evaluate whether the PrP^{Sc}–ferritin complex remains intact after transcytosis across Caco-2 cells, filter inserts containing Caco-2 cell monolayers were placed in a 12-well dish containing M17 neuroblastoma cells cultured on glass coverslips in the BL chamber (Fig. 6*A*, diagram). Subsequently, 20 μl of CJDH-DE or biotinylated CJDH-DE was added to the AP chamber. The biotinylated sample was used to distinguish added PrP and ferritin from endogenous proteins expressed by M17 cells. After an overnight incubation, transcytosed PrP^{Sc} and ferritin that had been subsequently endocytosed by M17 cells in the BL chamber were detected by immunostaining (Fig. 7*A*). The presence of tight junctions in Caco-2 cell monolayers was confirmed by immuno-

staining for ZO-1 and by checking the transport of ^{3}H-inulin before and after incubation with CJDH-DE.

Immunostaining of Caco-2 monolayers for ZO-1 shows uniform staining, confirming the presence of tight junctions during the course of the experiment (Fig. 7*A*, panels 1, 5). Coimmunostaining of M17 cells for PrP (green) and ferritin (red) shows colocalization at several spots, indicating that some of the PrP^{Sc}–ferritin complexes remain intact even after transcytosis across Caco-2 cells (Fig. 7*A*, panels 2–4). Coimmunostaining of M17 cells for PrP (green) and streptavidin (red) (Fig. 7*A*, panels 6–8) confirms that the PrP signal is derived from the transcytosed, biotinylated CJDH-DE added to the AP chamber.

Electron microscopic analysis of the PrP^{Sc}–ferritin complex immunoprecipitated with 8H4 (as in Fig. 5*A*, lanes 9, 13) shows fibrillar material decorated with ferritin aggregates (Fig. 7*B*, top inset, arrows). When added to a monolayer of Caco-2 cells, the PrP^{Sc}–ferritin complex is seen in small and large phagocytic vesicles enclosed by a single membrane with the fibrillar material intact within these vesicles (Fig. 7*B*, top). Groups of these vesicles are subsequently transported out from the BL membrane and are seen within the pore of the Transwell membrane (Fig. 7*B*, bottom).

Together, the above data demonstrate that the PrP^{Sc}–ferritin complex is endocytosed together by Caco-2 cells and a significant proportion is transcytosed intact to the BL chamber, where it is endocytosed again by M17 cells.

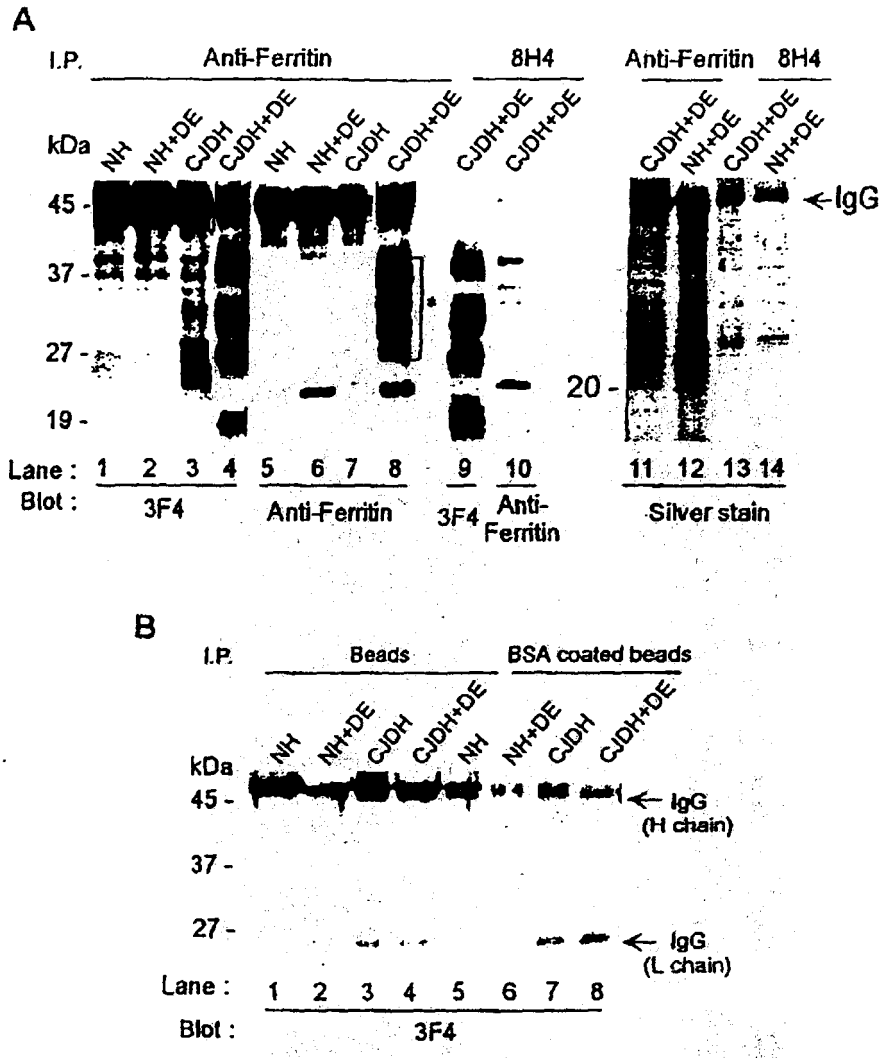

Figure 5. The PrP^{Sc}–ferritin complex coimmunoprecipitates with anti-ferritin and anti-PrP antibodies. Mock-treated or DE-treated NH and CJDH samples were immunoprecipitated (I.P.) with anti-ferritin or 8H4 antibodies, and coimmunoprecipitated proteins were detected by immunoblotting with specific antibodies. *A*, I.P. with anti-ferritin, followed by probing with 3F4, shows no coimmunoprecipitation of PrP^{C} from NH and NH-DE samples (lanes 1, 2). In contrast, full-length PrP^{Sc} and a significantly greater amount of protease-resistant PrP^{Sc} from CJDH and CJDH-DE immunoprecipitate with anti-ferritin (lanes 3, 4). Reprobing of the same membrane with anti-ferritin shows the H and L chains of ferritin migrating at 21 and 20 kDa in both NH and CJDH samples (lanes 5, 7). The H chain comigrates with the L chain at 20 kDa after DE treatment of NH and CJDH (lanes 6, 8). The identity of additional ferritin-immunoreactive bands in the CJDH-DE sample is unclear (lane 8, *). I.P. of CJDH-DE with 8H4, followed by probing with 3F4, shows PrP^{Sc} bands similar to the ones detected with anti-ferritin I.P. (compare lanes 9, 4). Reprobing with anti-ferritin reveals the 20 kDa ferritin band (lane 10). Silver staining of proteins immunoprecipitated with anti-ferritin or 8H4 shows bands comigrating with ferritin at 20 kDa and several other minor species (lanes 11–14). Note that the IgG band in 8H4 immunoprecipitates is negligible because the antibody was conjugated to protein A beads. A similar conjugation of anti-ferritin reduced the amount of coimmunoprecipitated PrP^{Sc} significantly. *B*, No PrP bands are detected in the absence of primary antibody either with protein A beads or BSA-coated protein A beads (lanes 1–8).

The binding of sCJD–PrP^{Sc} to Caco-2 cells is partially inhibited by excess ferritin

The persistent association of PrP^{Sc} with ferritin before and after transcytosis led us to investigate whether ferritin acts as a facilitator or a mediator of PrP^{Sc} transport across Caco-2 cells. Accordingly, an attempt was made to competitively inhibit the binding of PrP^{Sc} by preincubating Caco-2 cells with increasing amounts of purified ferritin to saturate available ferritin-binding sites. Two different PrP^{Sc} preparations were used for this purpose: (1) partially denatured biotin-tagged PrP^{Sc} isolated from CJDH that copurifies with ferritin after ultracentrifugation; and (2) biotin-tagged PrP^{Sc}–ferritin in its native conformation in CJDH-DE. For competition, three different preparations were used: (1) pure human liver ferritin; (2) pure human spleen ferritin; and (3) brain ferritin purified from NH (NH^{Pellet}).

Biotin-tagged PrP^{Sc} was purified by subjecting biotinylated CJDH to PK treatment and repeated rounds of ultracentrifugation, as in Figure 4. A sample from biotinylated NH was subjected to similar treatment, and the resulting pellet fractions from NH (NH^{Pellet}) and CJDH ($CJDH^{Pellet}$) were evaluated by Western blotting and silver staining. As expected, immunoblotting with 3F4 shows no reactivity with the NH sample and strong reactivity with N-terminally truncated PK-resistant PrP^{Sc} bands in the CJDH sample (Fig. 8*A*, lanes 1, 2). Reprobing of the membrane with anti-ferritin antibody shows the presence of ferritin in both NH and CJDH samples (Fig. 8*A*, lanes 3, 4). Longer exposure shows the presence of PrP^{Sc} and ferritin oligomers, despite treatment with DTT and boiling in SDS sample buffer (Fig. 8*A*, lanes 5–8, arrows). Silver staining of an aliquot from each sample

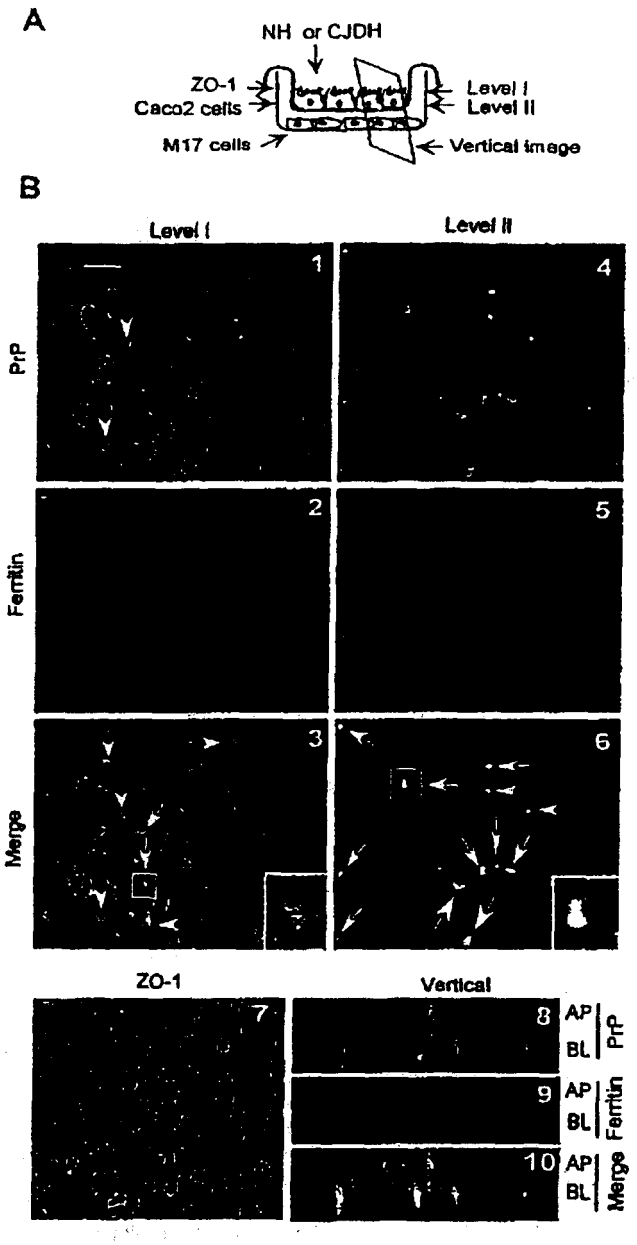

Figure 6. sCJD–PrP^{Sc} is cotransported with ferritin across Caco-2 cells. *A*, Diagrammatic representation of filter inserts with Caco-2 cell monolayers and the levels at which images were captured. M17 cells were cultured on glass coverslips in the BL chamber to capture transcytosed PrP^{Sc}–ferritin complexes (see Fig. 7*A*). *B*, Caco-2 cell monolayers were incubated with CJDH-DE in the AP chamber for 2 hr, and the filters were cut into two pieces. One was immunostained with 8H4–anti-mouse FITC (green) and anti-ferritin–anti-rabbit RITC (red) (panels 1–6), and the other was immunostained with with anti-ZO-1–anti-rabbit FITC (green) (panel 7). A horizontal image at level I shows colocalization of PrP (green) and ferritin (red) on the AP surface of Caco-2 cells (panels 1–3, arrows). Some PrP immunoreaction without ferritin is also seen (green) (panels 1–3, arrowheads). A horizontal image captured at level II shows colocalization of PrP (green) and ferritin (red) at the filter pores (panels 4–6, arrows). Immunostaining for ZO-1 shows the presence of tight junctions throughout the monolayer (panel 7). A vertical section through the Caco-2 monolayer shows similar colocalization of PrP (green) and ferritin (red) at the AP and BL membranes, as observed in the horizontal images (panels 8–10). Scale bar: 10 μm; inset, 2.5×.

showed ferritin in the NH^{Pellet} and ferritin along with PrP^{Sc} in the $CJDH^{Pellet}$ samples, as in Figure 4 (data not shown).

To check whether the purified preparations bind to Caco-2 cells and whether this binding can be competitively inhibited by ferritin, NH^{Pellet} and $CJDH^{Pellet}$ fractions were resuspended in purified human brain lipids lacking all proteins and sonicated to obtain a homogeneous mixture. Subsequently, polarized monolayers of Caco-2 cells were exposed to increasing amounts of NH^{Pellet}– and $CJDH^{Pellet}$–brain lipid mixture diluted in PBS containing 1% BSA for 30 min on ice and processed for staining with Texas Red–streptavidin. Remarkably, cells exposed to both NH^{Pellet} and $CJDH^{Pellet}$ show significant binding as determined by biotin-specific reactivity (Fig. 8*B*, panels 1, 2, −Ferritin). Under the experimental conditions used, 16 μl of NH^{Pellet}– and $CJDH^{Pellet}$–brain lipid preparation gave a reproducible and specific signal of defined intensity and was used for competition experiments. Thus, cells were exposed to 0, 0.5, 1.0, and 1.5 μg/ml human spleen ferritin resuspended in PBS containing 1% BSA for 30 min on ice, washed, and reexposed to 16 μl of NH^{Pellet} and $CJDH^{Pellet}$ for an additional 30 min on ice. The amount of streptavidin-reactive material bound to Caco-2 cells was determined by staining with Texas Red–streptavidin. Under these experimental conditions, 1.5 μg/ml pure spleen ferritin inhibits the binding of NH^{Pellet} and $CJDH^{Pellet}$ by ~80%, as determined by comparing the mean fluorescence intensity in 20 different fields (Fig. 8*B*, panels 3, 4, +Ferritin). Anti-ferritin- and PrP-specific antibodies were not used in this experimental setup because immunoreactivity is lost because of DTT treatment. The brain lipid used as vehicle did not show any reaction by itself (data not shown).

The binding of NH^{Pellet} that comprises only human brain ferritin and $CJDH^{Pellet}$ that comprises partially denatured PrP^{Sc} and ferritin and the inhibition of this binding by purified spleen ferritin suggest strongly that the binding of the PrP^{Sc}–ferritin complex to Caco-2 cells is mediated by ferritin, not by PrP^{Sc}.

Similar competition experiments were performed with biotin-tagged PrP^{Sc} in CJDH-DE, a milieu in which it maintains reactivity to the anti-PrP antibody 8H4. The inhibition of PrP^{Sc} binding in the presence of saturating amounts of ferritin was assessed by double staining with 8H4 and Texas Red–streptavidin. Although significant inhibition (~85%) of PrP^{Sc} binding is observed in the presence of 1.5 μg/ml spleen ferritin, we did not observe a complete block (Fig. 8*C*, panels 1–6, −Ferritin and +Ferritin). Similar results were obtained when liver ferritin was used as a competitive inhibitor (data not shown).

Our inability to demonstrate >80–85% inhibition of PrP^{Sc} binding despite high concentrations of free ferritin as a competitor led us to conclude that liver and spleen ferritin may not be the optimal inhibitors. Because ferritin in NH^{Pellet} is similar to the ferritin in CJDH-DE in terms of the source and method of preparation, we used NH^{Pellet} to saturate available ferritin-binding sites on Caco-2 cells before adding CJDH-DE. Thus, Caco-2 cells were exposed to 16 μl of NH^{Pellet}–brain lipid suspension for 30 min on ice, washed, and incubated for an additional 30 min on ice with 25 μl of CJDH-DE. The cells were then immunostained with 8H4 to detect bound PrP^{Sc}. Preincubation of the cells with 16 μl of NH^{Pellet} inhibited the binding of PrP^{Sc} by ~90% (Fig. 8*D*, panels 1, 2, $-NH^{Pellet}$ and $+NH^{Pellet}$).

Together, the above results suggest strongly that ferritin plays a significant role in the binding and transport of the PrP^{Sc}–ferritin complex across Caco-2 cells.

Discussion

This report provides insight into the pathway of PrP^{Sc} uptake and transport across intestinal epithelial cells. In particular, our data show that exposure of sCJD brain homogenate to DEs generates a C-terminal PrP^{Sc} core of 27–30 kDa that is transported across

Caco-2 cells in vesicular structures and that this process is not influenced by the level of endogenous PrP^C expression. Within these vesicles, PrP^{Sc} is associated with ferritin, a major component of the PrP^{Sc}–protein complex, and remains associated with ferritin after transcytosis. Because ferritin is normally absorbed from food and is abundantly present in a typical meat dish, these findings have important implications for prion uptake from contaminated food.

Using the well tested *in vitro* model for evaluating intestinal uptake of selected food nutrients (Cereijido et al., 1978; Pinto et al., 1983; Glahn et al., 1998), we show the resilience of PrP^{Sc} to DEs and the facilitative effect of such treatment on PrP^{Sc} uptake by Caco-2 cell monolayers. We noted that after treatment of CJDH with stomach pepsin, PrP^{Sc} underwent limited proteolysis and comigrated with the C-terminal PK-resistant core of PrP^{Sc}. Under similar conditions, PrP^C in the NH was completely hydrolyzed. Much to our surprise, DE-treated PrP^{Sc} was transported across Caco-2 cells four times more efficiently than PK-treated PrP^{Sc}. We believe that this effect is attributable to the chaotropic effect of bile salts that disperse PrP^{Sc}-containing membrane phospholipds into small micelles, preventing the aggregation of PrP^{Sc} and facilitating its binding to epithelial cells. This observation has significant practical implications because there could be qualitative and/or quantitative differences in the digestive process between individuals and certainly between different species. Such differences, although subtle and apparently trivial, may influence host susceptibility to prion infection from contaminated food.

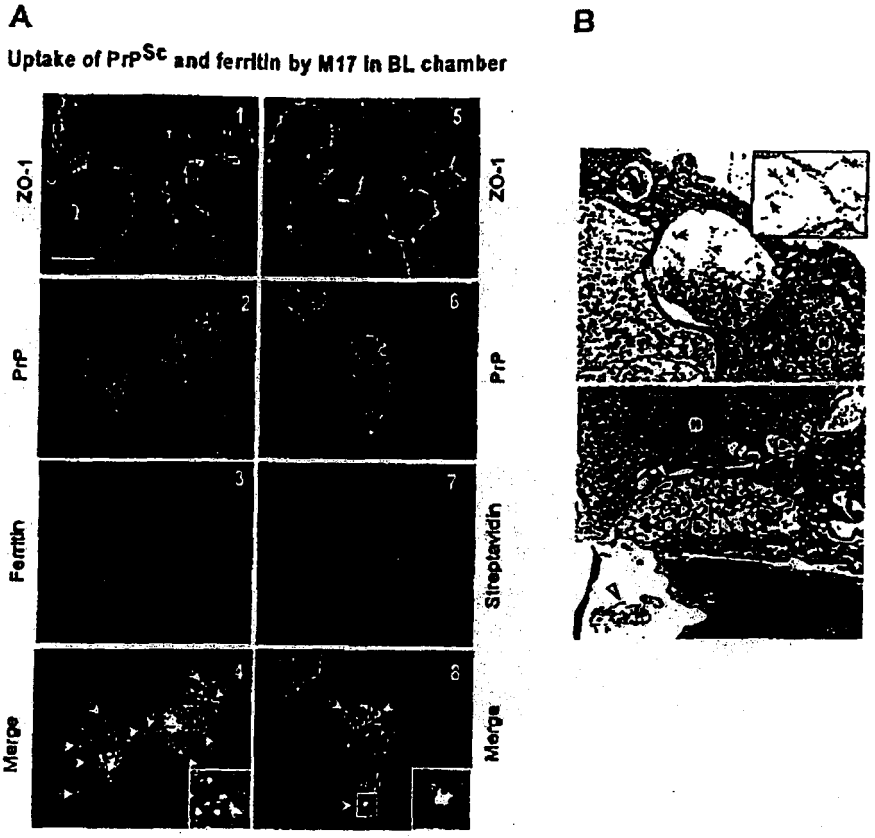

Figure 7. *sCJD–PrP^Sc remains associated with ferritin after transcytosis. A, Caco-2 cell monolayers were placed in a 12-well culture dish containing M17 neuroblastoma cells cultured on coverslips in the BL chamber, and biotinylated CJDH-DE was added to the AP chamber (see Fig. 6A). After an overnight incubation, Caco-2 cells on filters and M17 cells on coverslips were processed for immunostaining. Immunoreaction of filters with anti-ZO-1 shows the presence of tight junctions in all monolayers (green; panels 1, 5). Immunostaining of M17 cells in the BL chamber for PrP (green) and ferritin (red) shows colocalization of the two proteins, indicating the presence of intact PrP^Sc–ferritin complexes after transcytosis (panels 2–4, arrows). Coimmunostaining of M17 cells for PrP (green) and streptavidin (red) (panels 6–8) confirms that the PrP signal is derived from biotinylated CJDH-DE in the AP chamber. Scale bar, 10 μm. B, Electron microscopic analysis of the PrP^Sc–ferritin complex immunoprecipitated with 8H4 shows fibrillar structures and membranes decorated with ferritin aggregates (top inset; arrows). When added to Caco-2 cells, the complex is internalized in relatively large phagosome-like structures surrounded by a single membrane (top; arrowheads). Some of these vesicular structures are extruded out from the BL surface of Caco-2 cells and are seen within the pore of the membrane filter (bottom; arrowhead). (The internalized material in phagosomes shows similar structures as observed in the immunoprecipitated material.) Scale bar: 0.25 μm; inset, 1.5×. N, Nucleus; T, tight junction.*

While purifying PrP^{Sc} from CJDH, we noted that the H and L chains of ferritin consistently cosediment with PrP^{Sc}. Resistance of the PrP^{Sc}–ferritin complex to elution with low concentrations of salt and coimmunoprecipitation with either anti-PrP or anti-ferritin antibodies suggested an association between the two proteins, rather than coincidental sedimentation. Remarkably, both the H and L chains of ferritin resisted PK and DE treatment and were associated with the protease-resistant core of PrP^{Sc}. Electron microscopic examination of the 8H4-immunoprecipitated material revealed fibrils decorated with ferritin aggregates. Although other proteins were detected by silver staining of 8H4 and anti-ferritin immunoprecipitates attesting to the remarkably sticky nature of PrP^{Sc}, we believe that the association of PrP^{Sc} with ferritin is stronger and is more likely to be of biological significance. This notion is based on the fact that after repeated rounds of ultracentrifugation, only ferritin remained associated with PrP^{Sc}, and the complex could be dissociated only with 0.4 M NaCl. None of the other proteins copurified with PrP^{Sc}, suggesting that their coimmunoprecipitation with PrP^{Sc} is perhaps attributable to nonspecific interactions with the antibodies or with PrP^{Sc} itself (N. Morel et al., 2004). Whether the association of PrP^{Sc} and ferritin occurs *in vivo* or after homogenization of brain tissue is unclear from our data. Nevertheless, this complex is biologically significant because ingested PrP^{Sc} in contaminated meat undergoes a process similar to homogenization and DE treatment in the GI tract and is likely presented to the intestinal epithelium in a complex with ferritin. Interestingly, the β-sheet-rich PrP peptide 106–126 mixed with normal or CJD homogenate was not transcytosed effectively, indicating that the main determinant of PrP^{Sc} transport is not its β-sheet-rich secondary structure. Preincubation of PrP106–126, NH, or CJDH with exogenous purified ferritin did not facilitate the formation of coimmunoprecipitable PrP–ferritin complexes, indicating that the association of PrP^{Sc} with ferritin is more complex than a mere hydrophobic interaction during the process of homogenization. Regardless of the nature and site of PrP^{Sc}–ferritin complex formation, this phenomenon is likely to influence the absorption of ingested PrP^{Sc} significantly, especially because ferritin in ingested food is known to undergo active absorption by the human intestinal epithelium (Murray-Kolb et al., 2003; Theil, 2003).

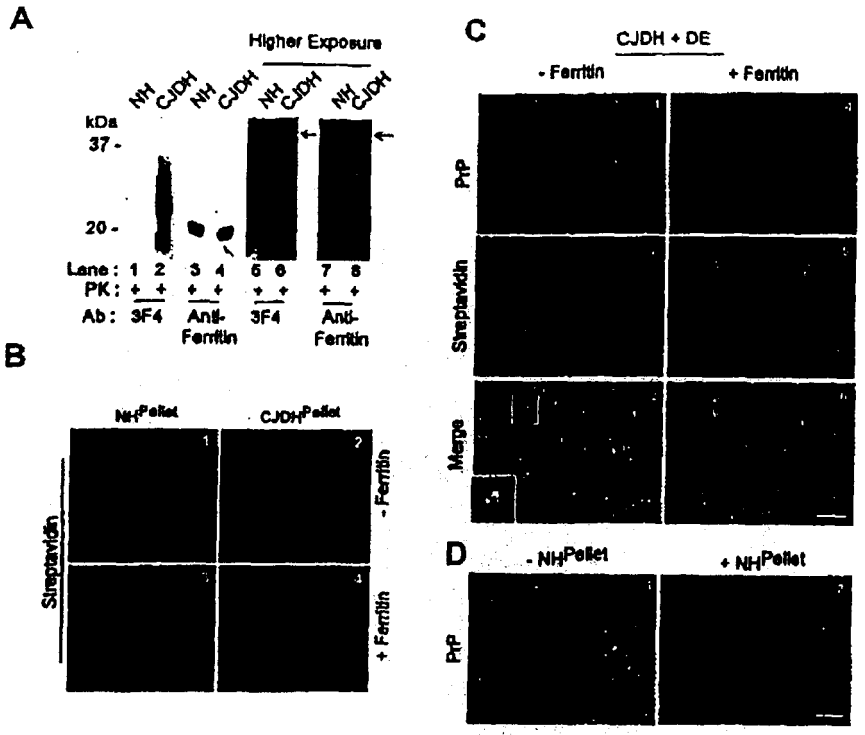

Figure 8. The binding of sCJD–PrP^{Sc}–ferritin to Caco-2 cells is competitively inhibited by excess ferritin. *A*, Western blotting of NH^{Pellet} and $CJDH^{Pellet}$ fractions with 3F4 reveals no reactivity with the NH sample but strong reactivity with N-terminally truncated PrP^{Sc} bands from the $CJDH^{Pellet}$ sample (lanes 1, 2). Reblotting with anti-ferritin shows the presence of ferritin in both NH and CJDH samples (lanes 3, 4). Longer exposure reveals high molecular weight bands of PrP and ferritin that appear to comigrate (lanes 5–8, arrow). *B*, Caco-2 cell monolayers were incubated with biotin-tagged NH^{Pellet}– or $CJDH^{Pellet}$–brain lipid mixture and processed for staining with Texas Red–streptavidin. Both NH^{Pellet} and $CJDH^{Pellet}$ bind to the cell surface (panels 1, 2, −Ferritin), and the binding is inhibited by preincubation of the cells with 1.5 μg/ml human spleen ferritin (panels 3, 4, +Ferritin). *C*, Caco-2 cells were incubated with 25 μl of biotinylated CJDH-DE with no previous exposure to ferritin (−Ferritin) or after preincubation with 1.5 μg/ml human spleen ferritin (+Ferritin) and processed for staining with Texas Red–streptavidin and 8H4–anti-mouse FITC (panels 1–6). Mock-treated cells show PrP-specific immunoreactivity (green) that colocalizes with streptavidin (red) (panels 1–3). However, preincubation with ferritin abolishes PrP-specific staining significantly (panels 4–6). *D*, Caco-2 cells with no previous treatment (panel 1, $-NH^{Pellet}$) or after preincubation with NH^{Pellet}–brain lipid mixture containing human brain-derived ferritin (panel 2, $+NH^{Pellet}$) were exposed to 25 μl of CJDH-DE and immunostained with 8H4–anti-mouse FITC. Mock-treated cells show strong PrP-specific immunoreactivity (panel 1), which is lost significantly after pretreatment of the cells with NH^{Pellet} (panel 2). Scale bar, 10 μm.

Our data show that 30–40% of ferritin from NH is consistently transcytosed across Caco-2 cells without degradation. In CJDH, this amount varies with the size of PrP^{Sc}-ferritin aggregates. Small, detergent soluble complexes are transcytosed intact, whereas large, detergent insoluble aggregates remain on the monolayer in the AP chamber (R. S. Mishra and N. Singh, unpublished observations). These large aggregates may be internalized via M-cells, follicular dendritic cells, or bone marrow-derived dendritic cells as reported previously (Heppner et al., 2001; Huang et al., 2002). It is conceivable that endocytosed ferritin is packaged in distinct vesicles that are either targeted to lysosomes or transcytosed to the BL surface. The associated PrP^{Sc} in CJDH probably follows both routes, although the majority appears to be transcytosed because very little PrP^{Sc} was detected in cell lysates (S. Basu and Singh, unpublished observations). This assumption is supported by the fact that a significant proportion of the PrP^{Sc}–ferritin complex remains intact after transcytosis, as evidenced by coimmunostaining of endocytosed aggregates in M17 cells cultured in the BL chamber. PrP^{C} from untreated NH did not show significant association with ferritin and was not transported to the BL chamber in several experiments. However, ferritin from untreated NH was detected consistently in the BL chamber (Basu and Singh, unpublished observations). Thus, either PrP^{C} is not endocytosed at all or is degraded within Caco-2 cells. A small amount of PrP^{Sc} was detected occasionally independent of associated ferritin. It is unclear whether this fraction is associated with another protein, is transported independently, or results from dissociation of the PrP^{Sc}–ferritin complex in an intracellular compartment.

Our results show that the PrP^{Sc}–ferritin complex is endocytosed by Caco-2 cells in vesicular structures that fuse to form phagosomes within the cell. Some of these vesicles are transcytosed intact to the BL chamber, much like the reported release of PrP^{Sc}-containing exosomes into the extracellular environment by epithelial cells (Fevrier et al., 2004). Sensitivity of the PrP^{Sc}–ferritin transport to incubation at low temperature and treatment with brefeldin A and nocodazole suggest the involvement of an active transport process (Klausner et al., 1992). Although Caco-2 cells are known to endocytose ferritin, the mechanistic details of this process remain elusive (Murray-Kolb et al., 2003). Specific receptors for ferritin have been reported on liver cells, lymphocytes, erythroblasts, oligodendrocytes, and on various cell lines (Mack et al., 1983; Harrison and Arosio, 1996; Hulet et al., 2000). Our data demonstrating significant inhibition of PrP^{Sc}–ferritin uptake in the presence of excess ferritin derived from human liver, spleen, or brain suggests the presence of a ferritin-specific receptor or a transporter on Caco-2 cells. The presence of such a receptor on epithelial cells and the close association of PrP^{Sc} and ferritin in digested food incriminate ferritin as a possible transporter of PrP^{Sc} across the intestinal epithelial cell barrier.

The notion that PrP^{Sc} is cotransported with ferritin ignores the key requirements of host susceptibility to prion infection, such as the level of PrP^{C} expression and the extent of homology between host PrP^{C} and incoming PrP^{Sc} (Prusiner et al., 1990; Weissmann et al., 2002; Thackray et al., 2003). Although in apparent contradiction, our data suggest that the uptake of PrP^{Sc} and its subsequent replication are distinct processes. The former is independent of host PrP^{C}, whereas the latter requires PrP^{C} as substrate for additional replication. This hypothesis is supported by our data that show no influence of PrP^{C} overexpression on PrP^{Sc} transport across Caco-2 cells and by a recent report demonstrating PrP^{C} expression below the tight junctions of polarized epithelial cells, making it physically impossible for incoming PrP^{Sc} to come in contact with host PrP^{C} (E. Morel et al., 2004).

The cotransport of PrP^{Sc} with ferritin raises important questions regarding prion uptake from contaminated food. Although this report uses a homologous experimental setup, ferritin H and L chains are known to share significant homology across species (Harrison and Arosio, 1996) and may facilitate the transport of

PrP^{Sc} from distant species across the intestine. Because PrP^{Sc} is notorious for its sticky nature, ferritin may be only one such carrier protein. The identification and functional role of other proteins associated with DE-treated PrP^{Sc} is important for fully understanding the mechanism of PrP^{Sc} uptake from ingested food and preventing a carrier state across species. Heterologous PrP^{Sc} in such carriers may be transported to sites where it may undergo conformational "adaptation" with time (Hill et al., 2000; Race et al., 2001), or in the case of livestock, lie dormant until ingested by a susceptible host. Such apparently "healthy" carriers would disseminate PrP^{Sc} through a variety of means, posing a potential threat to the general population.

References

Aguzzi A, Polymenidou M (2004) Mammalian prion biology: one century of evolving concepts. Cell 116:313–327.

Baron GS, Caughey B (2003) Effect of glycosylphosphatidylinositol anchor-dependent and -independent prion protein association with model raft membranes on conversion to the protease-resistant isoform. J Biol Chem 278:14883–14892.

Beekes M, McBride PA (2000) Early accumulation of pathological PrP in the enteric nervous system and gut-associated lymphoid tissue of hamsters orally infected with scrapie. Neurosci Lett 278:181–184.

Bons N, Mestre-Frances N, Belli P, Cathala F, Gajdusek DC, Brown P (1999) Natural and experimental oral infection of nonhuman primates by bovine spongiform encephalopathy agents. Proc Natl Acad Sci USA 96:4046–4051.

Cereijido M, Robbins ES, Dolan WJ, Rotunno CA, Sabatini DD (1978) Polarized monolayers formed by epithelial cells on a permeable and translucent support. J Cell Biol 77:853–880.

Collinge J (1999) Variant Creutzfeldt-Jakob disease. Lancet 354:317–323.

Fevrier B, Vilette D, Archer F, Loew D, Faigle W, Vidal M, Laude H, Raposo G (2004) Cells release prions in association with exosomes. Proc Natl Acad Sci USA 101:9683–9688.

Foster JD, Parnham DW, Hunter N, Bruce M (2001) Distribution of the prion protein in sheep terminally affected with BSE following experimental oral transmission. J Gen Virol 82:2319–2326.

Glahn RP, Lee OA, Yeung A, Goldman MI, Miller DD (1998) Caco-2 cell ferritin formation predicts nonradiolabeled food iron availability in an in vitro digestion/Caco-2 cell culture model. J Nutr 128:1555–1561.

Gu Y, Verghese S, Mishra RS, Xu X, Shi Y, Singh N (2003a) Mutant prion protein-mediated aggregation of normal prion protein in the endoplasmic reticulum: implications for prion propagation and neurotoxicity. J Neurochem 84:10–22.

Gu Y, Hinnerwisch J, Fredricks R, Kalepu S, Mishra RS, Singh N (2003b) Identification of cryptic nuclear localization signals in the prion protein: implications for prion disease pathogenesis. Neurobiol Dis 12:133–149.

Haik S, Faucheux BA, Sazdovitch V, Privat N, Kemeny J-L, Perret-Liaudet A, Hauw J-J (2003) The sympathetic nervous system is involved in variant Creutzfeldt-Jakob disease. Nat Med 9:1121–1123.

Harrison PM, Arosio P (1996) The ferritins: molecular properties, iron storage function and cellular regulation. Biochim Biophys Acta 1275:161–203.

Heppner FL, Christ AD, Klein MA, Prinz M, Fried M, Kraehenbuhl J-P, Aguzzi A (2001) Transepithelial prion transport by M cells. Nat Med 7:976–977.

Hill AF, Sidle KC, Joiner S, Keyes P, Martin TC, Dawson M, Collinge J (1998) Molecular screening of sheep for bovine spongiform encephalopathy. Neurosci Lett 255:159–162.

Hill AF, Joiner S, Linehan J, Desbruslais M, Lantos PL, Collinge J (2000) Species-barrier-independent prion replication in apparently resistant species. Proc Natl Acad Sci USA 97:10248–10253.

Huang FP, Farquhar CF, Mabbott NA, Bruce ME, MacPherson GG (2002) Migrating intestinal dendritic cells transport PrP^{Sc} from the gut. J Gen Virol 83:267–271.

Hulet SW, Heyliger SO, Powers S, Connor JR (2000) Oligodendrocyte progenitor cells internalize ferritin via clathrin-dependent receptor mediated endocytosis. J Neuron Res 61:52–60.

Klausner RD, Donaldson JG, Lippincott-Schwartz J (1992) Brefeldin A: insights into the control of membrane traffic and organelle structure. J Cell Biol 116:1071–1080.

Mack U, Powell LW, Halliday JW (1983) Detection and isolation of a hepatic membrane receptor for ferritin. J Biol Chem 258:4672–4675.

McBride PA, Schulz-Schaeffer WJ, Donaldson M, Bruce M, Diringer H, Kretzschmar HA, Beekes M (2001) Early spread of scrapie from the gastrointestinal tract to the central nervous system involves autonomic fibers of the splanchnic and vagus nerves. J Virol 75:9320–9327.

Miller MW, Williams ES (2003) Prion disease: horizontal transmission in mule deer. Nature 425:35.

Mishra RS, Gu Y, Bose S, Verghese S, Kalepu S, Singh N (2002) Cell surface accumulation of a truncated fragment of transmembrane prion protein in GSS P102L. J Biol Chem 277:24554–24561.

Morel E, Fouquet S, Chateau D, Yvernault L, Frobert Y, Pincon-Raymond M, Chambaz J, Pillot T, Rousset M (2004) The cellular prion protein PrP^{c} is expressed in human enterocytes in cell-cell junctional domains. J Biol Chem 279:1499–1505.

Morel N, Simon S, Frobert Y, Volland H, Mourton-Gilles C, Negro A, Sorgato MC, Creminon C, Grassi J (2004) Selective and efficient immunoprecipitation of the disease-associated form of the prion protein can be mediated by nonspecific interactions between monoclonal antibodies and scrapie-associated fibrils. J Biol Chem 279:30143–30149.

Murray-Kolb LE, Welch R, Theil EC, Beard JL (2003) Women with low iron stores absorb iron from soybeans. Am J Clin Nutr 77:180–184.

Nicotera P (2001) A route for prion neuroinvasion. Neuron 31:345–348.

Pan T, Colucci M, Wong BS, Li R, Liu T, Petersen RB, Chen S, Gambetti P, Sy MS (2001) Novel differences between two human prion strains revealed by two-dimensional gel electrophoresis. J Biol Chem 276:37284–37288.

Paramithiotis E, Pinard M, Lawton T, LaBoissiere S, Leathers VL, Zou W-Q, Estey LA, Lamontagne J, Lehto MT, Kondejewski L, Francoeur GP, Papadopoulos M, Haghighat A, Spatz SJ, Head M, Will R, Ironside J, O'Rourke K, Tonelli Q, Ledebur HC, et al. (2003) A prion protein epitope selective for the pathologically misfolded conformation. Nat Med 9:893–899.

Petersen RB, Parchi P, Richardson SL, Urig CB, Gambetti P (1996) Effect of the D178N mutation and codon 129 on the metabolism of the prion protein. J Biol Chem 271:12661–12668.

Peterson MD, Mooseker MS (1992) Characterization of the enterocyte-like brush border cytoskeleton of the C2BBe clones of the human intestinal cell line, Caco-2. J Cell Sci 102:581–600.

Pinto M, Robine-Leon S, Appay M-D, Kedinger M, Triadou N, Haffen K, Fogh J, Zweibaum A (1983) Enterocyte-like differentiation and polarization of the human colon carcinoma cell line Caco-2 in culture. Biol Cell 47:323–330.

Prinz M, Huber G, Macpherson AJS, Heppner FL, Glatzel M, Eugster H-P, Wagner N, Aguzzi A (2003) Oral prion infection requires normal numbers of Peyer's patches but not of enteric lymphocytes. Am J Pathol 162:1103–1111.

Prusiner SB (1998) Prions. Proc Natl Acad Sci USA 95:13363–13383.

Prusiner SB, Scott M, Foster D, Pan KM, Groth D, Mirenda C, Torchia M, Yang SL, Serban D, Carlson GA (1990) Transgenetic studies implicate interactions between homologous PrP isoforms in scrapie prion replication. Cell 63:673–686.

Race R, Raines A, Raymond GJ, Caughey B, Chesebro B (2001) Long-term subclinical carrier state precedes scrapie replication and adaptation in a resistant species: analogies to bovine spongiform encephalopathy and variant Creutzfeldt-Jakob disease in humans. J Virol 75:10106–10112.

Safar J, Wille H, Itri V, Groth D, Serban H, Torchia M, Cohen FE, Prusiner SB (1998) Eight prion strains have PrP^{Sc} molecules with different conformations. Nat Med 4:1157–1165.

Taylor DM (2002) Current perspectives on bovine spongiform encephalopathy and variant Creutzfeldt-Jakob disease. Clin Microbiol Infect 8:332–339.

Thackray AM, Klein MA, Bujdoso R (2003) Subclinical prion disease induced by oral inoculation. J Virol 77:7991–7998.

Theil EC (2003) Ferritin at the crossroads of iron and oxygen metabolism. J Nutr 133:1549S–01553S.

Weissmann C, Enari M, Klöhn P-C, Rossi D, Flechsig E (2002) Transmission of prions. Proc Natl Acad Sci USA 99:16378–16383.